Supplementary Information

Removal of Organophosphorus Agents *via* Atomically Dispersed Co on Nitrogen-Doped Graphene: Catalytic Degradation and Adsorption

Yanfang Li, Jiali Zhang,* Puyi Lei, and Shouwu Guo*

Department of Electronic Engineering, School of Electronic Information and Electrical

Engineering, Shanghai Jiao Tong University, Shanghai 200240, P. R. China.

*Correspondence should be addressed to: swguo@sjtu.edu.cn, zhangjiali@sjtu.edu.cn
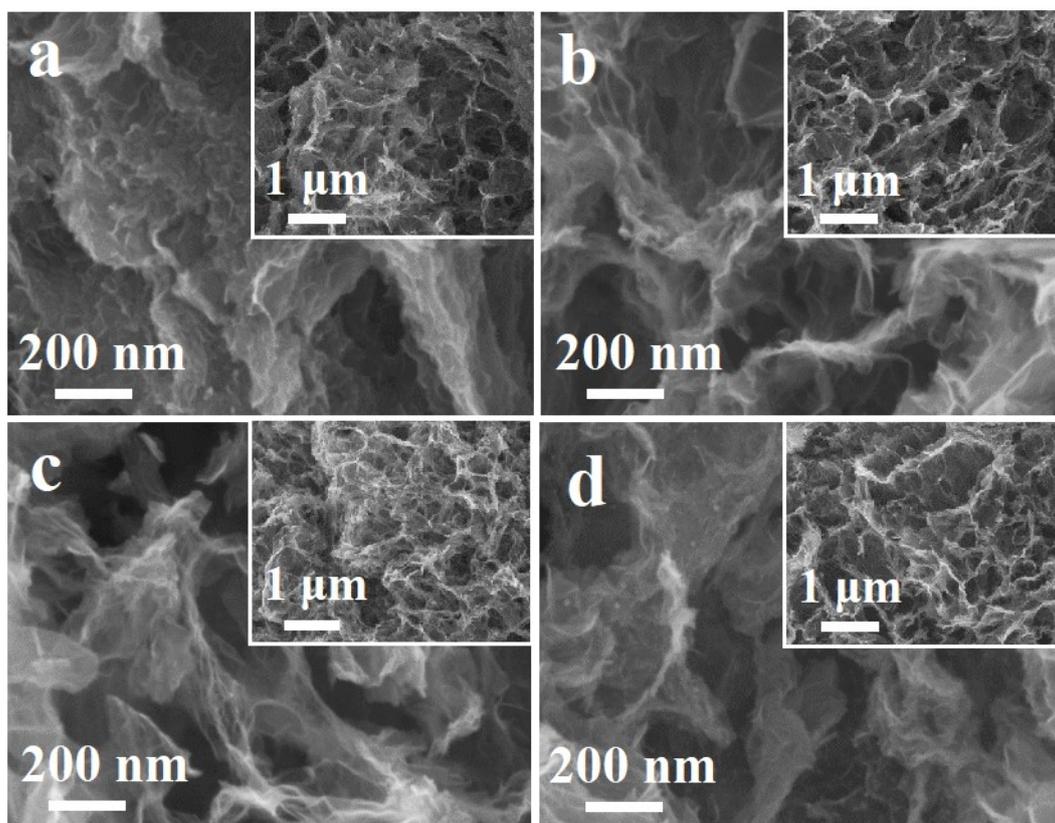
Figure S1. SEM images of ACo/3DNG$_{700}$ (a), ACo/3DNG$_{800}$ (b), ACo/3DNG$_{900}$ (c), and ACo/3DNG$_{1000}$ (d).
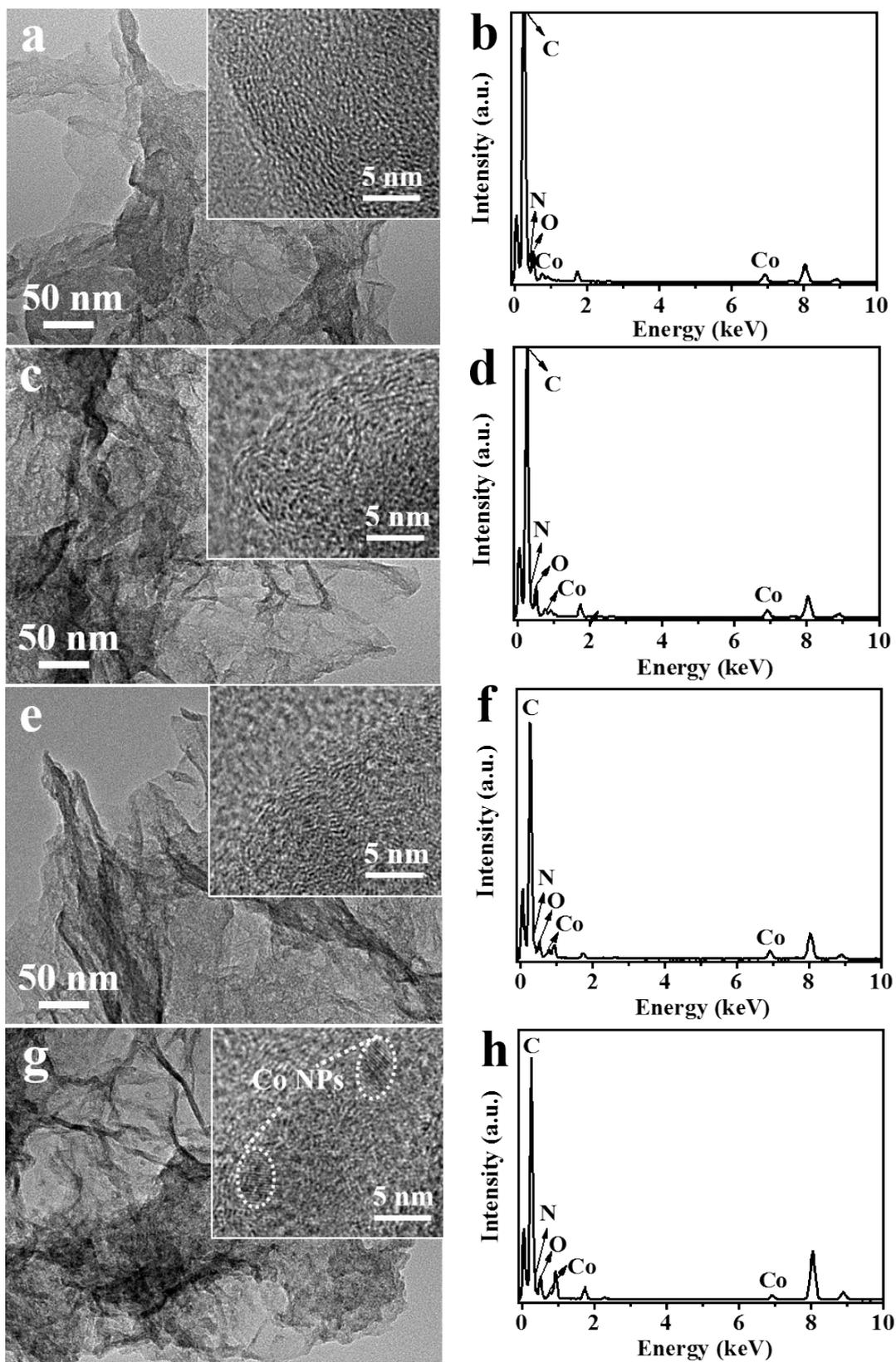
Figure S2. TEM and HRTEM images (inset), and the corresponding EDX spectra of the ACo/3DNG$_{700}$ (a, b), ACo/3DNG$_{800}$ (c, d), ACo/3DNG$_{900}$ (e, f), and ACo/3DNG$_{1000}$ (g, h).
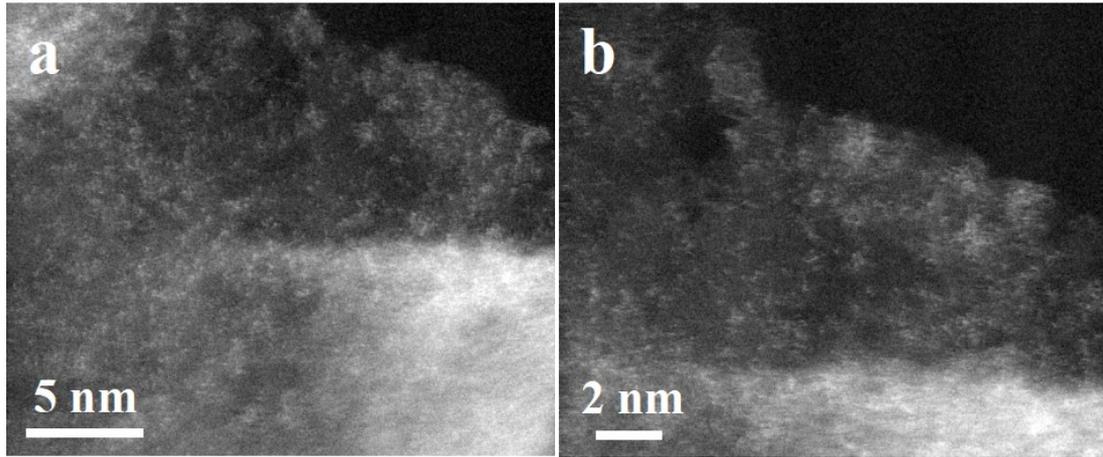
Figure S3. (a, b) AC-HAADF-STEM images of ACo/3DNG$_{800}$ at different magnifications.
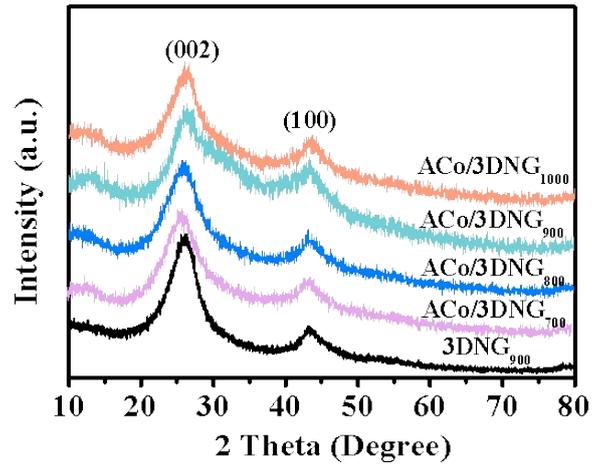
Figure S4. XRD patterns of $3DNG_{900}$, $ACo/3DNG_{700}$, $ACo/3DNG_{800}$, $ACo/3DNG_{900}$, and $ACo/3DNG_{1000}$.
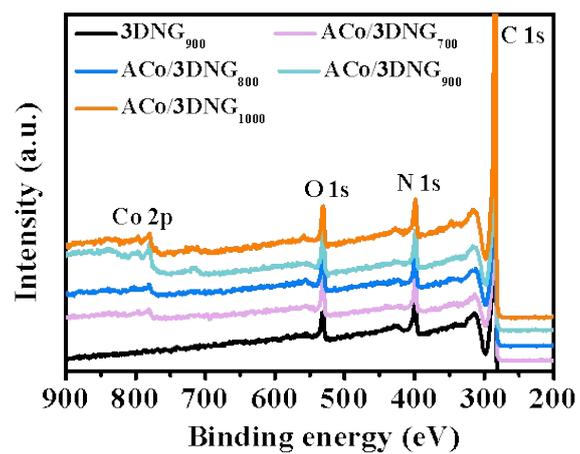
Figure S5. XPS spectra of $3DNG_{900}$, $ACo/3DNG_{700}$, $ACo/3DNG_{800}$, $ACo/3DNG_{900}$, and $ACo/3DNG_{1000}$.

Table S1. C, N, O, and Co contents (in weight) in different samples derived from the XPS spectra.

Samples	$3DNG_{900}$	$ACo/3DNG_{700}$	$ACo/3DNG_{800}$	$ACo/3DNG_{900}$	$ACo/3DNG_{1000}$
C/ %	89.02	84.20	84.57	85.17	87.19
N/ %	7.47	7.41	7.38	7.43	6.76
O/ %	3.52	6.42	5.70	5.32	3.98
Co/ %	0	1.97	2.05	2.08	2.07
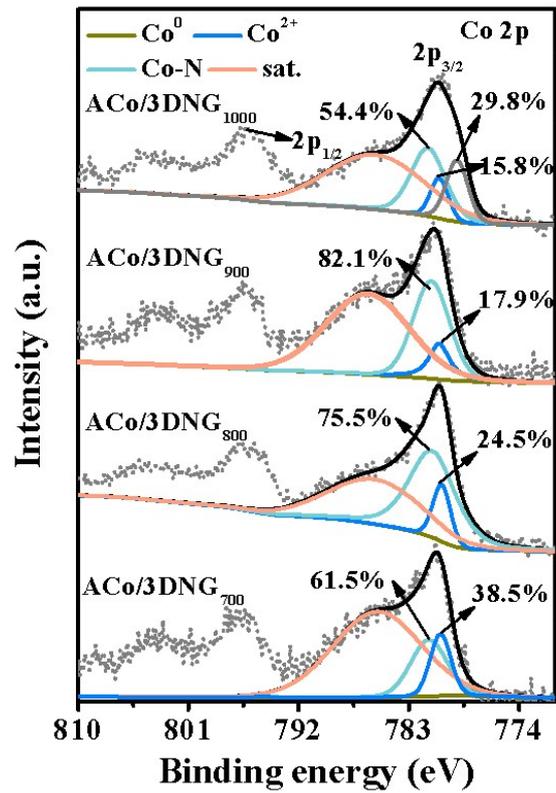
Figure S6. Hyperfine Co 2p XPS spectra of ACo/3DNG samples.
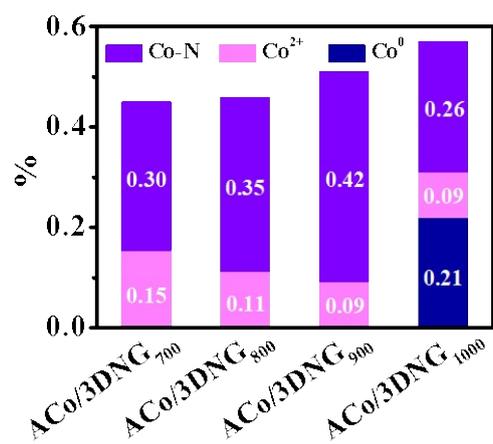
Figure S7. The mass content of the different Co species in ACo/3DNG composites.
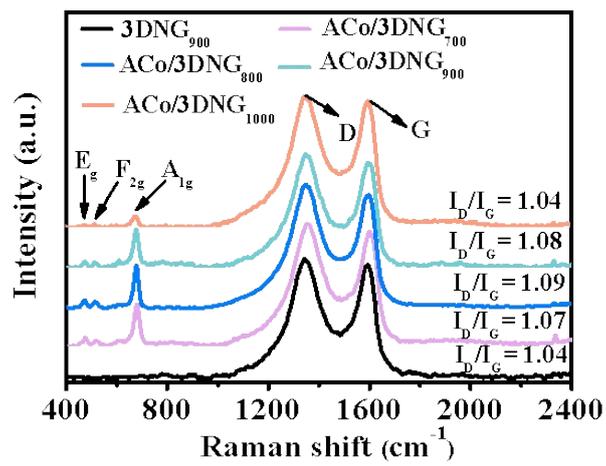
Figure S8. Raman spectra of 3DNG$_{900}$, ACo/3DNG$_{700}$, ACo/3DNG$_{800}$, ACo/3DNG$_{900}$, and ACo/3DNG$_{1000}$ composites.
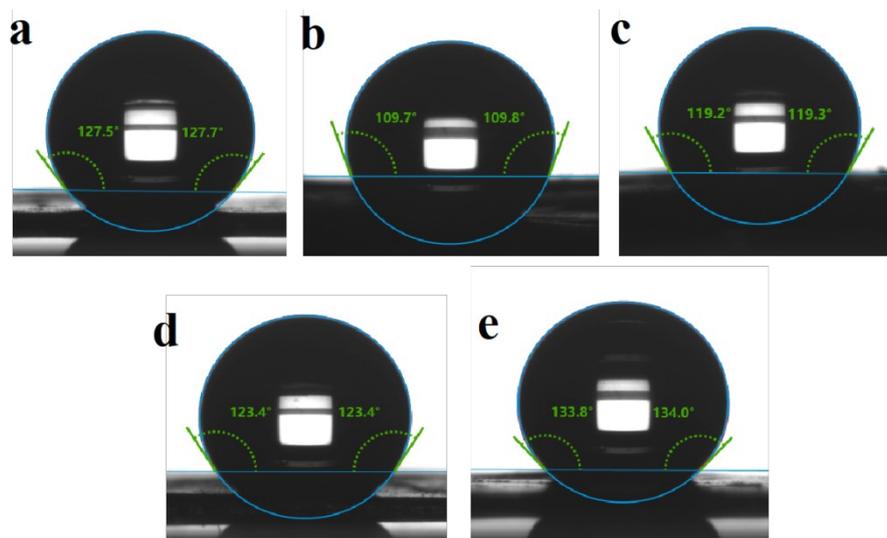
Figure S9. Water contact angle images of $3DNG_{900}$ (a), $ACo/3DNG_{700}$ (b), $ACo/3DNG_{800}$ (c), $ACo/3DNG_{900}$ (d), and $ACo/3DNG_{1000}$ (e), respectively.
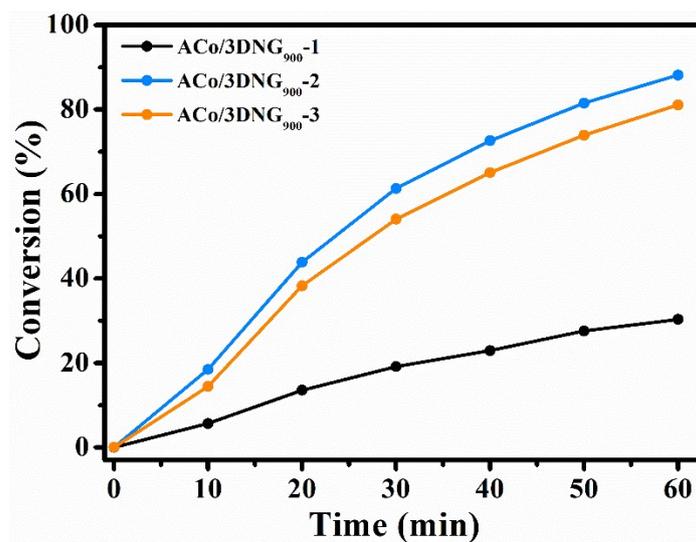
Figure S10. The catalytic activities of ACo/3DNG$_{900}$ with different Co loadings for hydrolysis of MP. The ACo/3DNG$_{900}$ with different Co loadings were prepared by tuning the Co(Ac)$_2$·4H$_2$O amount as follows: 5, 10, and 20 mg, respectively, corresponding to ACo/3DNG$_{900}$-1, ACo/3DNG$_{900}$-2, ACo/3DNG$_{900}$-3. The Co loadings of ACo/3DNG$_{900}$-1, ACo/3DNG$_{900}$-2 and ACo/3DNG$_{900}$-3 are of 2.0, 3.4, 4.2 wt%, determined by ICP-OES. Reaction condition: catalyst (200 μg), MP (100 μg), NH$_4$OH solution (2 mL, 50 mM), pH = 11.3, 20 °C.
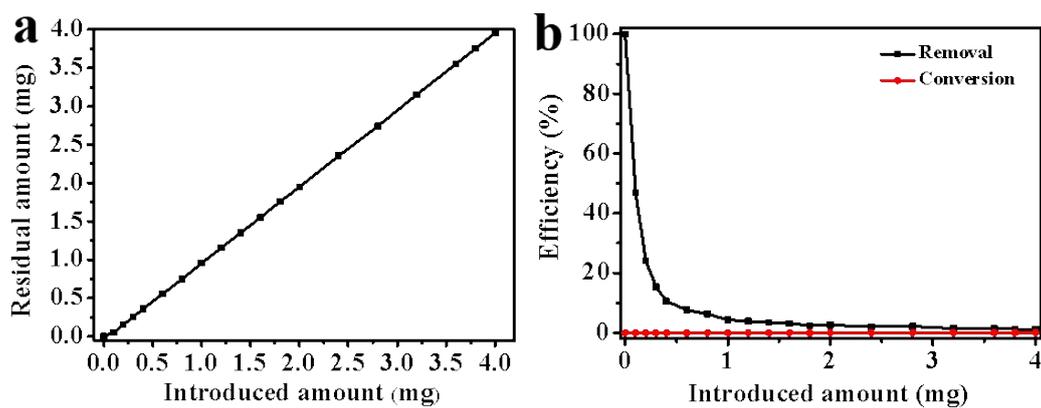
Figure S11. (a) The curve of the introduced amount vs residual amount of fenitrothion with pure silica gel column. (b) The catalytic degradation and removal performance of pure silica gel column for fenitrothion. Reaction condition: fenitrothion (4 mg), NH_4OH solution (50 mM), pH = 11.3, 20 ℃.
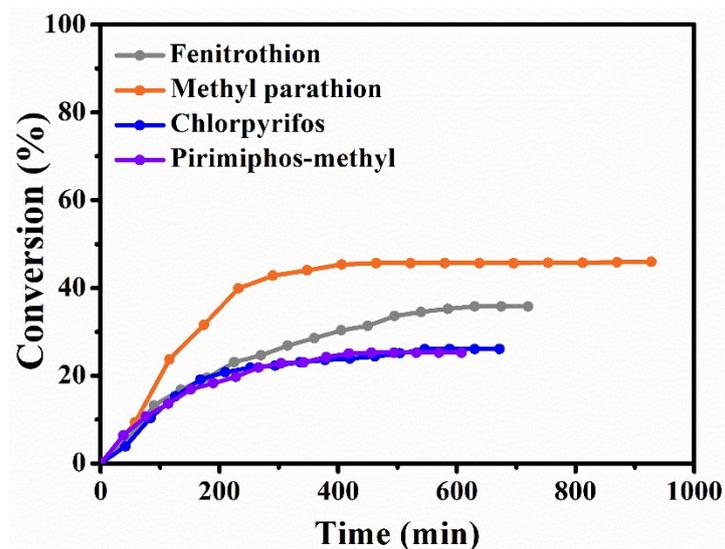
Figure S12. The conversion-time curves of different OPs pesticides on ACo/3DNG$_{900}$@Si column. Reaction condition: catalysts (2 mg), OPs pesticides (4 mg), NH$_4$OH solution (50 mM), pH = 11.3, 20 °C.
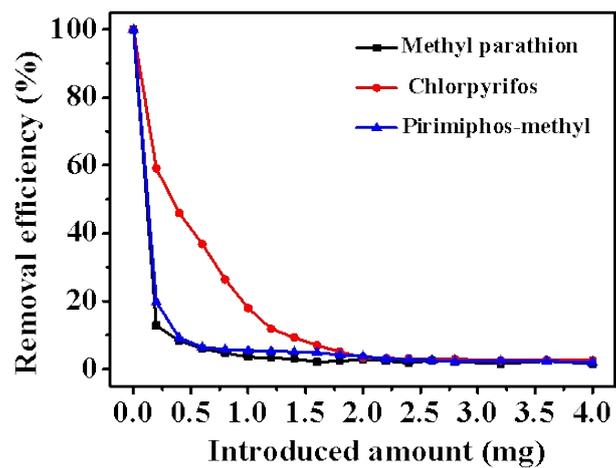
Figure S13. The removal performance of pure silica gel column for methyl parathion, chlorpyrifos, and pirimiphos-methyl, respectively. Reaction condition: OPs pesticides (4 mg), NH$_4$OH solution (50 mM), pH = 11.3, 20 °C.
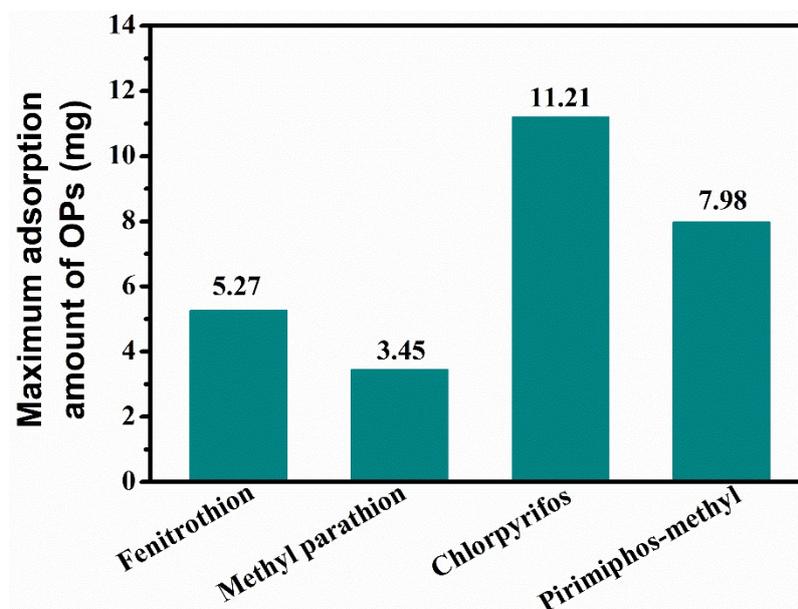
Figure S14. The maximum adsorption amounts of ACo/3DNG$_{900}$@Si column for OPs pesticides. Reaction condition: ACo/3DNG$_{900}$ (2 mg), NH$_4$OH solution (50 mM), pH = 11.3, 20 ºC.
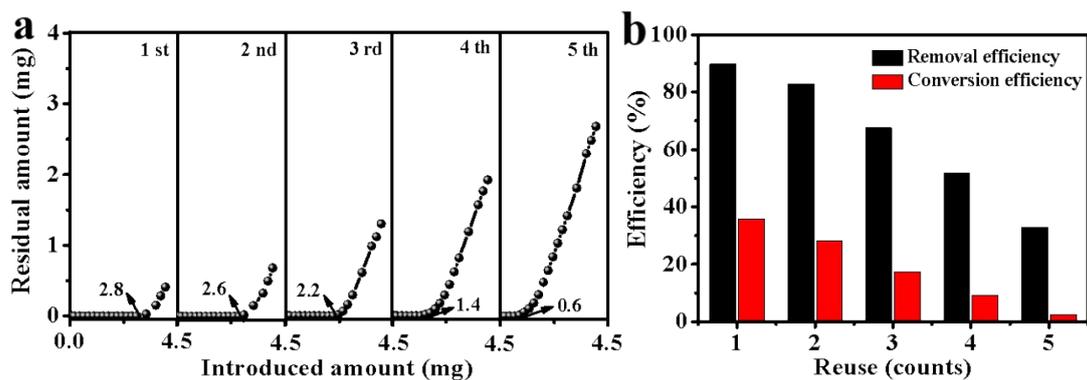
Figure S15. (a, b) Reusability of ACo/3DNG$_{900}$@Si column for continuous removal of fenitrothion. Reaction condition: ACo/3DNG$_{900}$ (2 mg), fenitrothion (4 mg), NH$_4$OH solution (50 mM), pH = 11.3, 20 °C.

Table S2. Mass content of C, N, O, and Co elements in ACo/3DNG$_{900}$ before and after use.

Samples	C/ %	N/ %	O/ %	Co/ %
ACo/3DNG$_{900}$ (before use)	85.17	7.43	5.32	2.08
ACo/3DNG$_{900}$ (after use)	84.84	6.57	7.33	1.26
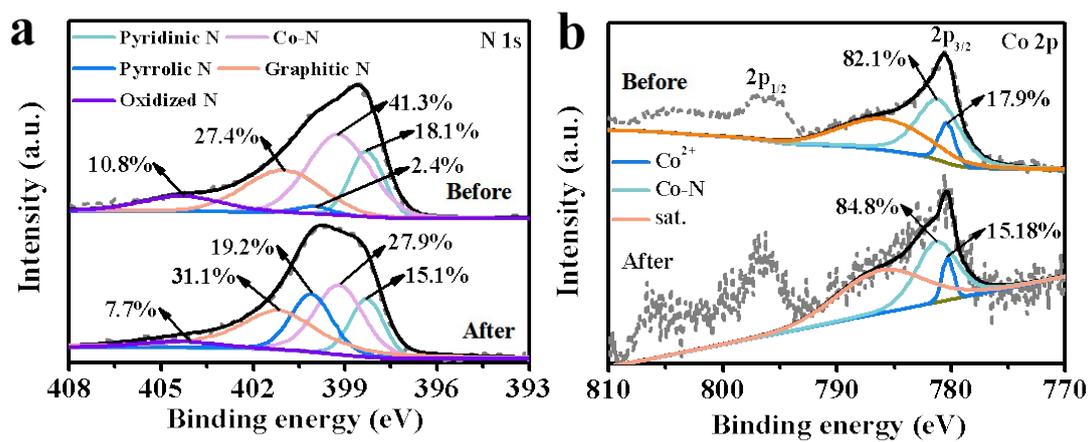
Figure S16. Hyperfine XPS spectra of N 1s (a) and Co 2p (b) of ACo/3DNG$_{900}$ in column before and after use.